An Experimental Model for Myocarditis and Congestive Heart Failure after Rabbit Coronavirus Infection

Suzanne Edwards, J. David Small, Joachim Dieter Geratz, Lorraine K. Alexander, and Ralph S. Baric

Department of Epidemiology, Program in Infectious Diseases, School of Public Health, and Department of Pathology, School of Medicine, University of North Carolina at Chapel Hill

In a model for virus-induced myocarditis and congestive heart failure, rabbit coronavirus infection was divided into acute (days 2–5) and subacute (days 6–12) phases on the basis of day of death and pathologic findings. During the acute phase, the principal histologic lesions were degeneration and necrosis of myocytes, myocytolysis, interstitial edema, and hemorrhage. The severity of these changes increased in the subacute phase. Pleural effusion and congestion of the lungs and liver were also present at this time. Myocarditis was detected by day 9 and peaked by day 12. Heart weights and heart weight–to–body weight ratios were increased, and dilation of the right ventricular cavity became prominent early in infection and persisted. In contrast, dilation of the left ventricle occurred late in the subacute stage. Virus was isolated from infected hearts between days 2 and 12. These data suggest that rabbit coronavirus infection progresses to myocarditis and congestive heart failure.

Viruses have long been recognized as important etiologic agents of heart disease in humans and experimental animals [1–3]. Epidemiologic evidence suggests that after viral infection, 2%–5% of a human population experience some degree of cardiac involvement [2, 3]. In humans and experimental animals, viruses commonly linked to heart disease include the picornaviruses, paramyxoviruses, myxoviruses, alphaviruses, and coronaviruses [2–5]. Viral infection of the heart may result in degeneration and necrosis of myocytes and lead to inflammation of the heart muscle. Myocarditis may result in arrhythmias, conduction disturbances, circulatory collapse, and acute congestive heart failure [3–7]. Acute viral infection of the heart muscle may also be an important factor in the development of idiopathic dilated cardiomyopathy [8–11].

Coxsackie B virus and encephalomyocarditis virus (both enteroviruses) infections in mice are the best-characterized model systems for virus-induced heart disease [1, 5]. The exact mechanism for their pathogenesis is still controversial; however, considerable evidence suggests that the disease is primarily immune-mediated rather than the result of direct viral cytotoxicity to myocytes [12, 13]. Both Coxsackie B and encephalomyocarditis virus infections in mice may progress to myocarditis and congestive heart failure, and some survivors may progress to a dilated cardiomyopathy later in life [5, 14–16]. The mechanisms by which viruses outside the enterovirus family cause heart disease are unclear.

A model for virus-induced cardiomyopathy has also been described in rabbits [17]. Rabbit cardiomyopathy is characterized by pulmonary edema, degeneration and necrosis of myocytes, and right ventricular dilation. Similar findings have also been reported in rabbits infected with pleural effusion disease virus [18, 19]. The etiologic agent for rabbit cardiomyopathy is probably a rabbit coronavirus (RbCV) antigenically related to the human coronavirus strain 229E [17]. We determined whether infection with RbCV would result in myocarditis and the development of congestive heart failure.

Materials and Methods

Animals and virus. Rabbit coronavirus (RbCV) was originally obtained from a stock maintained by one of the authors (J.D.S.). Viral stocks were diluted to 10^3–10^4 RID_{50}/ml and stored at −140°C. Male New Zealand white rabbits (Franklin Rabbitry, Wake Forest, NC), weighing 2.5–3.0 kg, were housed at room temperature (21–24°C) and given water and rabbit diet (Agway; Grandville Milling, Creedmoor, NC) ad libitum. The animals were inoculated intravenously via the marginal ear vein with 0.2 ml of the 10^3–10^4 RID_{50} viral stock. Body weight and rectal temperature were recorded daily. Animals were observed for signs of infection: dullness of the sclerae, severe congestion of the conjunctivae and irides, rectal temperatures >39°C, and weight loss.

To assay viral titers in the heart muscle, moribund animals were intravenously injected with 50 mg/kg sodium pentobarbitol, and the hearts were perfused and washed extensively with PBS. Two hundred micrograms of left ventricle were ground in 0.8 ml of PBS and centrifuged at 12,000 *g* for 10 min in an Eppendorf centrifuge (Fisher Scientific, Norcross, GA). The su-

Received 20 June 1991; revised 6 September 1991.

Presented in part: International Coronavirus Symposium, Cambridge, UK, July 1989.

Grant support: National Institutes of Health (AI-23946); American Heart Association (871135 and Established Investigator Award 890192 to R.S.B.).

Reprints or correspondence: Dr. Ralph S. Baric, Department of Epidemiology, School of Public Health, University of North Carolina at Chapel Hill, Chapel Hill, NC 27599-7400.

The Journal of Infectious Diseases 1992;165:134–40

0022-1899/92/6501-0018$01.00

pernatant was serially diluted and inoculated into the marginal ear vein of rabbits.

Histologic studies. Animals dying from RbCV infection were necropsied within 12 h of death. Alternatively, moribund animals were sacrificed as described above. Body weights were obtained to the nearest 0.10 kg. The heart was separated from the pericardial sac, trimmed of fat and extraneous tissue, and flushed with PBS. The heart was weighed to the nearest 0.1 g; the chambers were filled with 10% phosphate-buffered formalin (BF) and immersed in 10% BF for 24–48 h. The heart was removed and sectioned transversely at the widest dimensions of the ventricles. After additional fixation in BF, four paraffin-embedded 6-μm sections were cut at 150-μm intervals and stained with hematoxylin-eosin (H&E) stain. Selected sections were also stained by Masson's trichrome and the von Kossa stains. Sections of the lung, liver, thymus, kidney, and spleen were also stained with H&E.

Morphometric studies. A computerized Zeiss Videoplan-1 digital morphometric system (Carl Zeiss, Thornwood, NY) was used to measure the dimensions of the cardiac walls and cavities and to examine the area within each ventricular section. To measure the thickness of the right and left ventricular walls and interventricular septum, 15–20 measurements were taken at regular intervals across the ventricles. Two or three different cardiac sections were measured from each animal, and the standard deviations were calculated and recorded. The dimensions of the ventricular cavities were measured at 15–20 points across the midpoint in each ventricle and then averaged between three or four consecutive cross-sections in the same animal. Large differences between consecutive cross-sections were not detected. Papillary muscle projections complicated measurements of the left ventricular cavity and wall. Consequently, the area in each left and right ventricle cross-section was measured two or three times and averaged between different cross-sections in the same animal.

Animals dying during the acute or subacute phase of infection were grouped accordingly, and mean values were averaged and reported as mean ± SD. Student's *t* test for unpaired observations was used to evaluate the statistical significance of differences in cardiac dimensions.

Results

Mortality and course of RbCV infection. Fifty-four New Zealand white rabbits were inoculated with 0.2 ml of a 10^3–10^4 RID_{50}/ml stock and examined daily for clinical signs of infection. Consistent with earlier studies [17], mortality rates peaked at 4 days after infection, decreased, and then increased again between day 6 and 8. No animals died after 12 days after infection, and the overall mortality rate approached 64% (27% acute; 37% subacute) (figure 1).

Animals dying early from infection had enlarged hearts characterized by striking dilation of the right ventricular cavity and accompanied by pulmonary edema. Pleural effusion and congestion of the lungs and liver were occasionally present during the acute phase but were more commonly observed between days 6–9 after infection. Clinically, rabbits

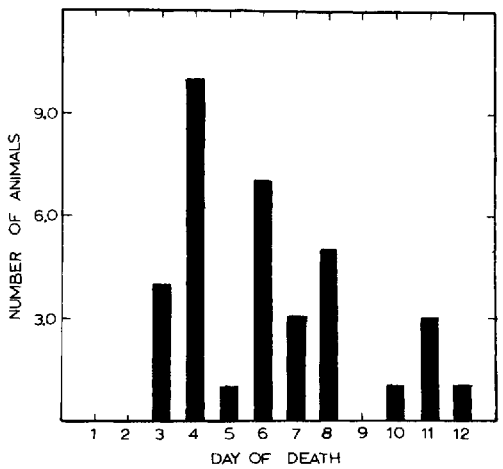

Figure 1. Mortality and course of rabbit coronavirus infection.

exhibited moist rales and wheezing during the subacute stage. Rabbits that died on days 10–12 had pleural effusion, pulmonary edema, ascites, enlarged hearts, dilated right and left ventricular cavities, and congestion in the lungs and liver. From these observations, we divided RbCV infection into an acute phase that was characterized by dilation of the right ventricle and pulmonary edema (days 2–5) and a subacute phase that was characterized by dilation of both ventricles and heart failure (days 6–12).

Heart weight and heart weight–to–body weight ratios during RbCV infection. Body weight, heart weight, and heart weight–to–body weight ratios were measured on days 2–5, when myocardial degeneration and necrosis and pulmonary edema became apparent, and days 6–12, when heart failure was evident. Body weights slowly decreased during the course of infection and were notably decreased (~0.4 kg) during the subacute phase of the disease (data not shown).

Control rabbits sacrificed on days 2–5 (acute, $n = 10$) or days 6–12 (subacute, $n = 10$) had heart weights of 6.1 ± 0.3 g and 6.1 ± 0.5 g, respectively. After RbCV infection, heart weights were significantly increased, to 8.4 ± 1.4 g during the acute stage ($n = 12$) ($P < .001$) and 8.7 ± 1.6 g during the subacute phase of infection ($n = 14$) ($P < .001$). Heart weight–to–body weight ratios were 0.0022 ± 0.0002 in the uninfected controls and were increased significantly, to 0.0031 ± 0.0003 ($P < .001$) and 0.0035 ± 0.0006 ($P < .001$) during the acute and subacute phases of infection, respectively.

Dimensions of the cardiac walls during RbCV infection. Changes in the size of the heart and, in particular, dimensions of the ventricles were evident after RbCV infection (figure 2). To conclusively document the anatomic changes in the heart during infection, the thickness of the ventricular wall was measured through the coronal axis at the midpoint of the ventricles.

The thickness of the right wall in uninfected controls was

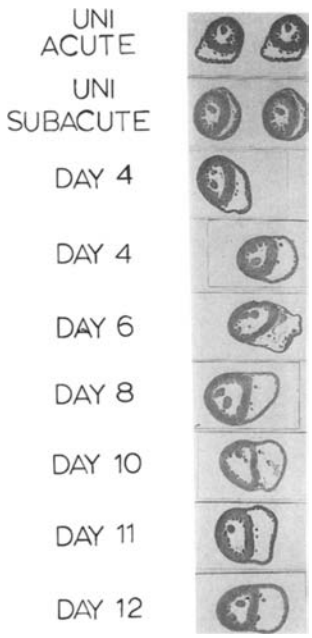

Figure 2. Progression of cardiac dilation during rabbit coronavirus infection: representative sections from days 4–12 after infection. Uninfected control (UNI) animals were sacrificed on comparable days.

~2100 μm (figure 3A). During the acute phase of infection, the thickness of the right ventricular wall decreased significantly, by ~25% compared with uninfected controls ($P < .001$). Significant thinning of the right ventricular wall continued through the subacute stage of infection ($P < .001$). The decrease amounted to ~37% compared with uninfected controls sacrificed on identical days. The most significant changes in the dimensions of the right wall were detected in animals dying 9–12 days after infection.

The thickness of the interventricular septum was 4470 ± 676 μm and 4470 ± 503 μm in uninfected controls sacrificed on days 3–5 and 6–12, respectively. The septum was 4419 ± 740 μm in animals dying during the acute stage of infection ($P = .875$). However, the thickness of the interventricular septum was decreased significantly, to 3597 ± 603 μm, during the subacute phase of the disease ($P = .002$).

The thickness of the left ventricular wall was also similar between the uninfected controls and animals dying during the acute phase of the disease ($P = .445$). However, the thickness of the left ventricular wall was significantly reduced, by ~15%, during the subacute phase ($P < .05$) (figure 3B).

Dimensions of the ventricular cavities during RbCV infection. In uninfected controls, the width of the right ventricular cavity was ~3100 μm (figure 4A). In infected animals, the width of the right ventricular cavity was significantly increased, by ~105% during the acute stage of infection ($P < .001$) and 177% during the subacute stage of infection ($P < .001$). Dimensions of the left ventricular cavity were not significantly different between the uninfected controls and the animals dying early in the infection ($P = .145$) (figure 4B). However, significant differences in the dimensions of the left cavity were noted during the subacute stage of infection ($P = .004$).

To obtain an additional estimate of the dilation of the right and left ventricular cavities during infection, we averaged the area in several consecutive right and left ventricular cavity sections from animals dying during the acute or subacute phase. Areas within the right and left ventricular cavity were similar between control animals sacrificed on days 3–5 or 6–12 (figure 5A, B). After RbCV infection, the area in the right ventricular cavity increased by ~150% during the acute stage ($P < .001$) and 254% during the subacute phase ($P < .001$) (Figure 5A). Areas within the left ventricular cavity were not altered significantly during the early stages of infection ($P = .278$), but significant increases, of ~30%, were noted during the subacute phase ($P = .025$) (figure 5B).

Pathologic findings during RbCV infection. Rabbits were divided into two groups according to the day of death and pathologic findings in the host. With minor variations, lesions were similar to those previously reported [17]. The heart was the principal target organ, often with red streaks present on the epicardial and endocardial surfaces. Pulmonary edema was always present, and accumulations of 10–30 ml of clear pale yellow fluid, which clotted on standing, were

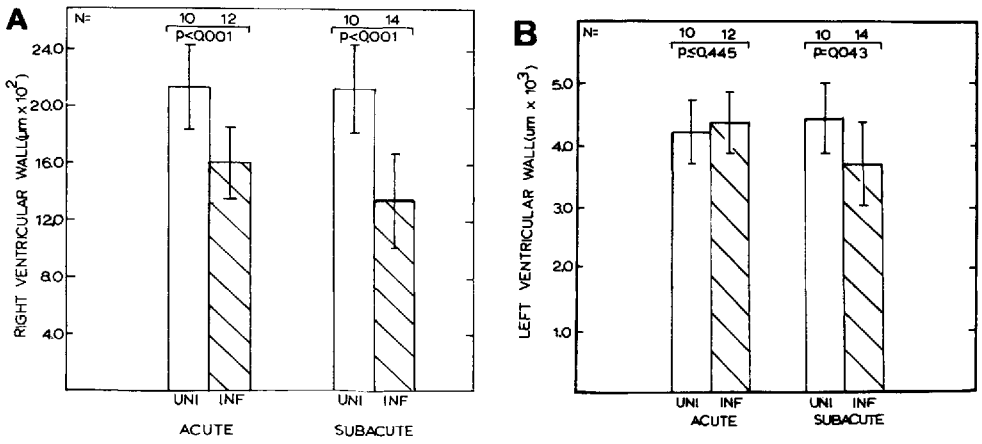

Figure 3. Dimensions of right (**A**) and left (**B**) ventricular walls during acute and subacute rabbit coronavirus infection (INF) compared with uninfected controls (UNI) sacrificed on similar days. Measurements are mean ± SD and were evaluated by Student's *t* test.

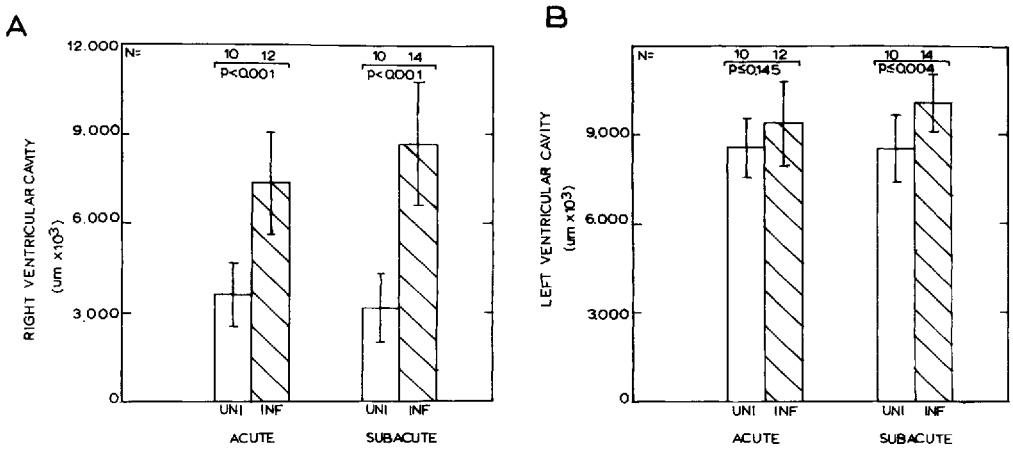

Figure 4. Dimensions of right (**A**) and left (**B**) ventricular cavities during acute and subacute rabbit coronavirus infection (INF) compared with uninfected controls (UNI). Measurements are mean ± SD and were evaluated by Student's *t* test.

often present in the thorax. The frequency and volume of pleural effusion increased during the subacute period. Late in the subacute period, a small amount of ascites fluid was seen in some animals. Accentuation of the hepatic lobules was present in some rabbits dying during the subacute period; however, the liver margins remained sharp.

Microscopically, myocardial lesions in rabbits dying during the acute phase consisted of widening of intercellular spaces, scattered infiltrates of small numbers of heterophiles (rabbit neutrophils), increased granularity of myocyte cytoplasm, hemorrhage, and occasional degeneration and necrosis of myocytes (figure 6A). Only rarely were foci of frank hemorrhage and calcification seen during this period. Lesions were seen equally in the right and left ventricles and in the interventricular septum. As rabbits survived beyond 5 days, lesions progressed in size, number, and maturity. In several rabbits, necrotic foci had varying degrees of calcification (figure 6B). Lesions were equally present in the left and right ventricles, interventricular septum, and papillary muscle. No lesions were seen in the heart valves or the vessels. Interstitial edema increased. In addition to increased numbers of heterophils, macrophages and lymphocytes were seen. Myocarditis was usually diffuse to focal and peaked by day 10–12 (figure 6C).

Alveolar epithelial cells were swollen. In a few rabbits of the subacute group, much of the intraalveolar fluid had been readsorbed, leaving fibrinous strands, macrophages, and heterophils. Interalveolar blood vessels were distended (figure 6D). Lymphoid tissue adjacent to bronchi was within normal limits, and bronchial epithelium was unremarkable.

Liver lesions were subtle during the acute phase. Sinusoids were slightly distended, especially in areas surrounding central veins. In several rabbits the first row or two of hepatocytes surrounding some of the central veins were rounded up, hyalinized with indistinct nuclei, and deeply eosinophilic. With increased time to death in the subacute stage,

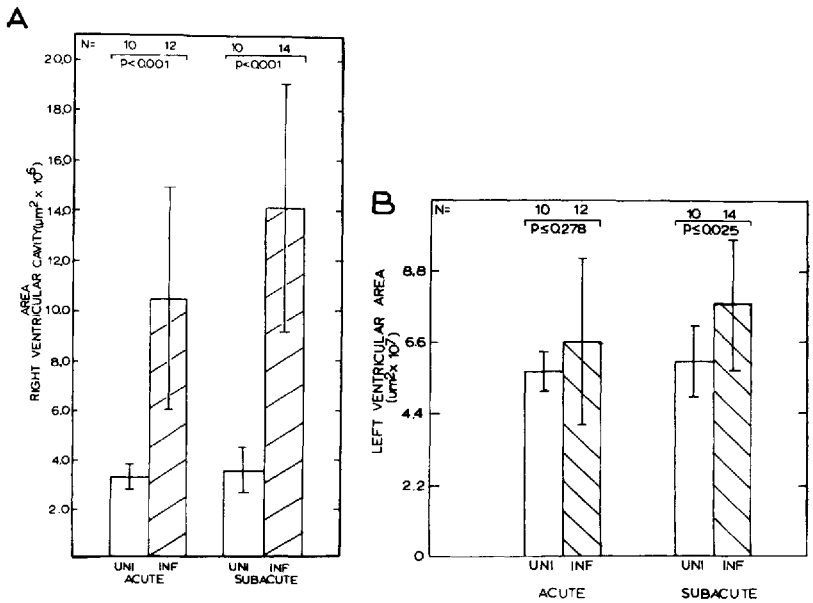

Figure 5. Area within right (**A**) and left (**B**) ventricular cavity during acute and subacute rabbit coronavirus infection (INF) compared with uninfected controls (UNI). Measurements are mean ± SD and were evaluated by Student's *t* test.

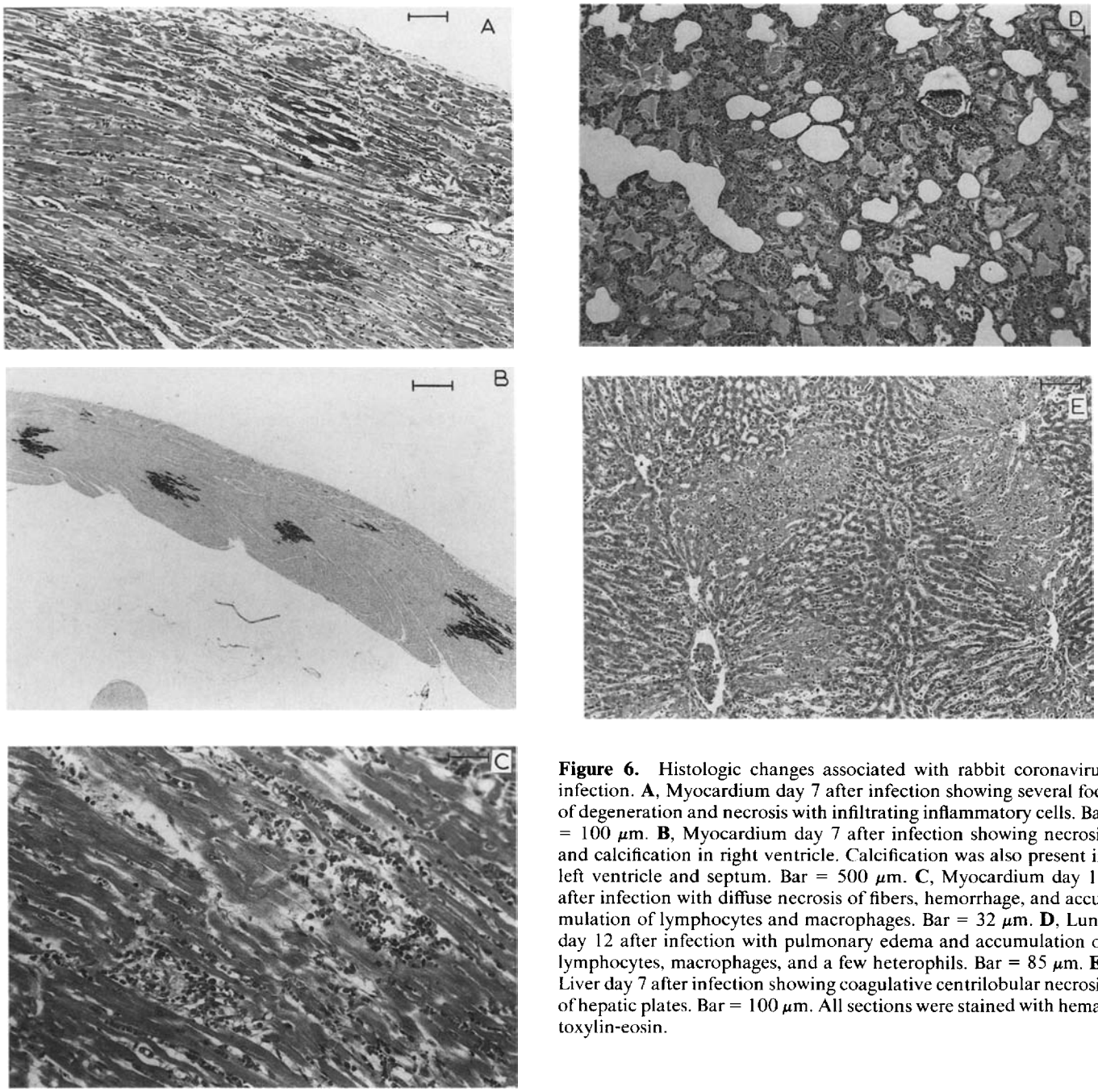

Figure 6. Histologic changes associated with rabbit coronavirus infection. **A**, Myocardium day 7 after infection showing several foci of degeneration and necrosis with infiltrating inflammatory cells. Bar = 100 μm. **B**, Myocardium day 7 after infection showing necrosis and calcification in right ventricle. Calcification was also present in left ventricle and septum. Bar = 500 μm. **C**, Myocardium day 10 after infection with diffuse necrosis of fibers, hemorrhage, and accumulation of lymphocytes and macrophages. Bar = 32 μm. **D**, Lung day 12 after infection with pulmonary edema and accumulation of lymphocytes, macrophages, and a few heterophils. Bar = 85 μm. **E**, Liver day 7 after infection showing coagulative centrilobular necrosis of hepatic plates. Bar = 100 μm. All sections were stained with hematoxylin-eosin.

sinusoids became more distended, individual hepatocytes were compressed, the number of hepatocytes undergoing coagulative necrosis around the central veins increased, and the necrotic areas became increasingly hypercellular. Portal triads were normal (figure 6E).

Isolation of infectious virus. Infectious virus was isolated from the hearts of animals dying between days 2 and 12. Virus was first detected in the heart muscle by day 2 (10^2–10^3 RID_{50}/g). Peak titers in the heart muscle occurred on days 3–5 (10^5–10^6 RID_{50}/g), and significant titers were detected through day 12 (10^2–10^3 RID_{50}/g). No virus was detected in the uninfected controls.

Discussion

Viral infection of the heart muscle may result in degeneration and necrosis of myocytes, myocarditis, and congestive heart failure [1–5, 7]. Viral infection may also be an important factor in the development of idiopathic dilated cardiomyopathy [5, 20–22]. The incidence and mechanisms by which

viruses cause heart disease in humans and animals are unclear, because these agents are rarely recovered from the patients and heart tissue at biopsy. Since many different viral infections may result in cardiac damage, model systems are needed to examine the basis for virus-induced heart disease.

RbCV infection results in degeneration and necrosis of myocytes, myocarditis, interstitial edema, hemorrhage, increased heart weight and heart weight–to–body weight ratios, and dilated ventricles. Although dry weights of the hearts were not determined, pathologic findings suggest that the increase in heart weight is probably caused by interstitial edema. Animals dying in the subacute stage of the disease develop congestion in the lungs and liver, suggesting that a significant percentage of these animals probably die from heart failure. Manifestations of both left- and right-sided heart failure are clearly evident in the subacute phase of infection [4, 6, 7, 21]. Previous studies in our laboratory clearly demonstrated the presence of viral antigen in regions of myocardial degeneration and infectious virus in the hearts of infected animals, supporting the idea that changes in the myocardium are most likely caused by viral replication in the heart muscle [17].

The pathogen for this disease is morphologically and antigenically related to the group I human and porcine coronaviruses [17]. RbCV is also related to the etiologic agent responsible for pleural effusion disease in rabbits [17–19, 23]. Both viruses have similar isolation histories and antigenic properties and produce similar diseases in vivo. Here we demonstrated that infection with RbCV results in myocarditis. Rabbits normally require 8–10 days to develop a strong lymphocytic infiltration after infection [24]. By the Dallas classification system [25], focal to diffuse myocarditis with fibrosis is clearly present by day 9 and reaches peak levels on days 10–12. In previous studies, little lymphocytic infiltration was noted because most of the animals dying from RbCV or pleural effusion disease virus infection were examined before day 9 [17, 18, 26]. It seems likely that pleural effusion disease virus infection also results in a significant percentage of animals dying from heart failure, since degeneration and necrosis of myocytes, pulmonary edema, pleural effusion, dilated ventricles, and congestion of the lungs, liver, and spleen are common [18, 26].

In humans, virus-induced myocarditis and congestive heart failure have been reported after infection with herpesvirus, enterovirus, paramyxovirus, myxovirus, alphavirus, flavivirus, and others [1–3, 27, 28]. Complications associated with coronavirus infections in humans include myocarditis and perimyocarditis [4]. During the subacute phase of infection, myocardial lesions observed in rabbits closely resemble those of acute myocarditis in humans. Lesions are distributed throughout the ventricles and consist of necrotic fibers surrounded by macrophages and lymphocytes. Adjacent areas of the myocardium appear normal. The endocardium and pericardium are spared. Later, necrotic fibers are replaced with connective tissue or calcification, and the number of macrophages and lymphocytes are reduced [1, 25].

The most extensively studied models for virus-induced myocarditis and congestive heart failure are in mice inoculated with enteroviruses (encephalomyocarditis virus or Coxsackie B virus) [1, 5, 21]. There are also model systems for influenza virus–induced metabolic alterations in the heart [29], reovirus-induced myocarditis in mice [30], and parvovirus-induced myocarditis in dogs [31]. In rabbits, poxvirus infections may also result in degeneration and necrosis of myocytes and myocarditis [32]. Rabbit coronavirus infection is similar to the encephalomyocarditis virus model. Early in that infection, animals are probably dying from acute heart failure caused by a complete atrioventricular block [15, 33]. In the subacute stage of infection, animals die from myocarditis-induced congestive heart failure [13, 15]. The most notable difference between the two models is that myocarditis, myocyte necrosis, and calcification appear to be much more extensive after encephalomyocarditis virus infection [14, 15].

In the case of encephalomyocarditis and Coxsackie B virus infections, maximum inflammation and cardiac necrosis occur after the clearance of virus from the heart, suggesting that direct viral cytotoxicity to myocytes is of limited importance [1]. Rather, the preponderance of data suggest that cardiac damage is immune-mediated [12, 13, 34–39]. The pathogenic mechanisms for myocyte injury after RbCV infection are unclear. Early in infection, significant myocyte damage correlates with high viral titers in the heart and occurs before the presence of significant inflammatory infiltrates. Heterophils and macrophages that are occasionally present early in infection probably represent a nonspecific response to necrotic cell injury. These data suggest that myocardial injury may initially result from direct viral infection, similar to findings reported early in canine parvovirus infection [31].

We have described a model system for virus-induced myocarditis and congestive heart failure in rabbits. These data provide the underlying foundation for future studies examining the mechanism of RbCV-induced heart disease in rabbits.

Acknowledgments

We thank Gillian Harris and Edna Lennon for excellent secretarial assistance and James E. Hall, Sheila Peel, Mary C. Schaad, and Robert E. Johnston for editorial comments.

References

1. Woodruff JF. Viral myocarditis. Am J Pathol **1980**;101:427–84.
2. Abelmann WH. Viral myocarditis and its sequelae. Annu Rev Med **1973**;24:145–52.
3. Abelmann WH. Virus and the heart. Circulation **1971**;44:950–6.
4. Riski H, Hovi T. Coronavirus infections of man associated with diseases other than the common cold. J Med Virol **1980**;6:259–65.

5. Kawai C, Matsumori A, Kitaura Y, Takatsu T. Viruses and the heart: viral myocarditis and cardiomyopathy. Prog Cardiol **1978**;7:141–62.
6. Bolte HD. Viral heart disease. New York: Springer-Verlag, **1984**.
7. Chung EK. Manual of acute cardiac disorders. Stoneham, MA: Butterworth, **1988**.
8. Braunwald E. Heart disease: a textbook of cardiovascular medicine. 3rd ed. Philadelphia: W. B. Saunders, **1988**.
9. Roberts WC, Ferrans VJ. Pathologic anatomy of the cardiomyopathies. Hum Pathol **1975**;6:287–342.
10. Oakley C. Diagnosis and natural history of congested (dilated) cardiomyopathies. Postgrad Med J **1978**;54:440–7.
11. Torp A. Incidence of congestive cardiomyopathy. Postgrad Med J **1978**;54:435–7.
12. Woodruff JF, Woodruff JJ. Involvement of T lymphocytes in the pathogenesis of Coxsackie virus B3 heart disease. J Immunol **1974**;113:1726–34.
13. Kishimoto C, Kuribayashi K, Masuda T, Tomioka N, Kawai C. Immunologic behavior of lymphocytes in experimental viral myocarditis: significance of T lymphocytes in the severity of myocarditis and silent myocarditis in BALB/C-nu/nu mice. Circulation **1985**; 71:1247–54.
14. Matsumori A, Kawai C. An animal model of congestive (dilated) cardiomyopathy: dilation and hypertrophy of the heart in the chronic stage in DBA/2 mice with myocarditis caused by encephalomyocarditis virus. Circulation **1982**;66:355–60.
15. Matsumori A, Kawai C. An experimental model for congestive heart failure after encephalomyocarditis virus myocarditis in mice. Circulation **1982**;65:1230–5.
16. Reyes MP, Ho KL, Smith F, Lerner AM. A mouse model of dilated-type cardiomyopathy due to coxsackievirus B3. J Infect Dis **1981**;144:232–6.
17. Small JD, Aurelian L, Squire RA, et al. Rabbit cardiomyopathy associated with a virus antigenically related to human coronavirus strain 229E. Am J Pathol **1979**;95:709–29.
18. Fennestad KL, Mansa B, Christensen N, Larsen S, Svehag SVE. Pathogenicity and persistence of pleural effusion disease virus isolates in rabbits. J Gen Virol **1986**;67:993–1000.
19. Fennestad KL, MacNaughton MR. Pleural effusion disease in rabbits. Properties of the aetiological agent. Arch Virol **1983**;76:179–87.
20. Rose AG, Beck W. Dilated (congestive) cardiomyopathy: a syndrome of severe cardiac dysfunction with remarkably few morphological features of myocardial damage. Histopathology **1985**;9:367–79.
21. Matsumori A, Kawai C. Animal models of congestive heart failure and congestive (dilated) cardiomyopathy due to viral myocarditis in mice. In: Bolte HD, ed. Viral heart disease. New York: Springer-Verlag, **1984**:35–56.
22. Cambridge G, MacArthur CGC, Waterson AP, Goodwin JF, Oakley CM. Antibodies to Coxsackie B virus in congestive cardiomyopathy. Br Heart J **1979**;41:692–6.
23. Fennestad KL. Pathogenetic observations on pleural effusion disease in rabbits. Arch Virol **1985**;84:163–74.
24. Lukehart SA, Baker-Zander SA, Lloyd RMC, Sell S. Effect of cortisone administration on host-parasite relationships in early experimental syphilis. J Immunol **1981**;127:1361–8.
25. Aretz HT, Billingham ME, Edwards WD, et al. Myocarditis, a histopathologic definition and classification. Am J Cardiol Pathol **1987**;1:3–14.
26. Fennestad KL, Skovgaard Jensen HJ, Moller S, Weis Bentzon M. Pleural effusion disease in rabbits. Clinical and post mortem observations. Acta Pathol Microbiol Scand [B] **1975**;83:541–8.
27. Obeyesekere I, Hermon Y. Myocarditis and cardiomyopathy after arbovirus infections (dengue and chikungunya fever). Br Heart J **1972**;34:821–7.
28. Jin Ou, Sole MJ, Butany JW, et al. Detection of enterovirus RNA in myocardial biopsies from patients with myocarditis and cardiomyopathy using gene amplification by polymerase chain reaction. Circulation **1990**;82:8–16.
29. Ilback NG, Friman G, Beisel WR, Johnson AJ. Sequential metabolic alterations in the myocardium during influenza and tularemia in mice. Infect Immun **1984**;45:491–7.
30. Sherry B, Fields BN. The reovirus M1 gene, encoding a viral core protein, is associated with the myocardic phenotype of a reovirus variant. J Virol **1989**;63:4850–6.
31. Meunier PC, Cooper BJ, Appel MJG, Slauson DO. Experimental viral myocarditis: parvoviral infection of neonatal pups. Vet Pathol **1984**;21:509–15.
32. Pearce JM. Susceptibility of the heart of the rabbit to specific infection in viral diseases. Arch Pathol **1942**;34:319–33.
33. Kishimoto C, Matsumori A, Ohmae M, Tomioka N, Kawai C. Electrocardiographic findings in experimental myocarditis in DBA/2 mice: complete atrioventricular block in the acute stage, low voltage of the QRS complex in the subacute stage and arrhythmias in the chronic stage. J Am Coll Cardiol **1984**;3:1461–8.
34. Huber SA, Lodge PA. Coxsackievirus B3 myocarditis. Identification of different pathogenic mechanisms in DBA/2 and BALB/c mice. Am J Pathol **1986**;122:284–91.
35. Huber SA, Lodge PA. Coxsackievirus B-3 myocarditis in BALB/C mice. Evidence for autoimmunity to myocyte antigens. Am J Pathol **1984**;116:21–9.
36. Huber SA, Job LP. Differences in cytolytic T cell response of BALB/C mice infected with myocarditic and nonmyocarditic strains of coxsackievirus group B, type 3. Infect Immun **1983**;39:1419–27.
37. Neu N, Beisel KW, Traystman MD, Rose NR, Craig SW. Autoantibodies specific for the cardiac myosin isoform are found in mice susceptible to coxsackievirus B3–induced myocarditis. J Immunol **1987**;138:2488–92.
38. Weller AH, Simpson K, Herzum M, vanHouten N, Huber SA. Coxsackievirus-B3-induced myocarditis: virus receptor antibodies modulate myocarditis. J Immunol **1989**;143:1843–50.
39. Saegusa J, Prabhakar BS, Essani K, et al. Monoclonal antibody to coxsackievirus B4 reacts with myocardium. J Infect Dis **1986**; 153:372–3.